MOF-composite sensors to eliminate the QCM positive frequency shift

Nicholaus Prasetya *, Salih Okur

Institute of Functional Interfaces (IFG), Karlsruhe Institute of Technology, Hermann-von-Helmholtz-Platz 1, 76344 Eggenstein-Leopoldshafen, Germany

ARTICLE INFO

Keywords:
Quartz crystal microbalance (QCM)
Metal organic frameworks (MOF)
Positive frequency
Stiffness

ABSTRACT

In a quartz crystal microbalance (QCM) Sauerbrey equation can usually be applied in the ideal scenario and when the QCM frequency shift goes to the negative direction. In some cases, however, the requirements to achieve the ideal condition are not fulfilled and thus leading to QCM positive frequency shift phenomenon. Herein we have also observed that a porphyrin-based metal organic frameworks (MOF), namely MOF-525(Zn), QCM sensor also exhibits the positive frequency shift phenomenon when exposed to xylene isomers, which could be caused by the loose attachment of the MOF nanoparticles on the QCM surface. Therefore, in the presence of the analytes, the bonding between the MOF and the QCM surface is disturbed and higher analyte concentration also leads to the increase of the sensitive layer stiffness, resulting in higher positive frequency shift. However, such a phenomenon can be completely eliminated by simply adding polymer to MOF nanoparticle sensors to strengthen the bonding of MOF nanoparticles to the QCM surface. Through this study we have shown that adjusting the amount of polymer is very crucial to completely reverse the positive frequency response. Otherwise, it appears a critical analyte concentration of gas analytes where the QCM frequency shift changes its direction from negative to positive response. Lastly, the same strategy has also been used to other MOF-based QCM sensor systems where their sensitive layer is built from other MOFs, namely MOF-525 and NU-902, and ethanol is used as the analyte to prove the generalizability of this simple approach.

1. Introduction

Quartz Crystal Microbalance (QCM) is a mass-sensitive transducer that works based on the inverse piezoelectric effect where an applied voltage on the QCM causes a mechanical vibration in the quartz crystal. QCM has then been widely used as a mass-sensitive sensor because of its high sensitivity, low cost and fast-response time [1]. When QCM is used as a mass-sensitive sensor, an inverse and linear relationship can usually be observed between the change of the analyte mass and the sensor frequency. Such a relationship has been well-described through Sauerbrey Eq. (1):

$$\Delta m = \frac{C_{QCM}}{n}\Delta f \tag{1}$$

in which Δm is the amount of adsorbed mass, C_{QCM} is the QCM mass sensitivity constant, n is the resonance frequency overtone and Δf is the change in the QCM frequency when an analyte is adsorbed on the QCM. However, this only occurs if the whole system of the QCM sensor, which consists of sensitive layers and analytes, can oscillate synchronously [2]. Therefore, to realize this objective, the sensitive layer should uniformly cover the QCM surface as a thin and rigid film [3]. If these requirements are not fulfilled, a deviation from the Sauerbrey equation could be observed and, in some cases, could also lead to the enhancement instead of the reduction of the crystal frequency as indicated by the positive frequency shift of the QCM [2,3]. There are then various factors that could cause this phenomenon such as the absence of a rigid and uniform QCM sensitive layer film, viscoelastic loading onto the QCM surface and the elasticity change of the sensitive layer during analyte adsorption process [3,4].

The phenomenon of the QCM positive frequency shift has then been reported in various cases. For example, this phenomenon has been observed in QCM sensors that are applied for humidity sensing. In this case, a number of different materials have been reported to construct the QCM sensitive layer that can induce such a behavior such as ZnO nanoparticles [5,6], ZnO nanowire [7], ZnS nanowire [4,8], polymer composites [9] and protonated polyethylenimine-graphene oxide nanocomposite [10]. A QCM positive frequency has also been observed in a sensor that was fabricated by using CuO nanostructures as the sensitive layer to detect trace amount of hydrogen cyanide gas [11]. In addition, this phenomenon is also observed when micron-sized

* Corresponding author.
E-mail address: nicholaus.prasetya@partner.kit.edu (N. Prasetya).

polyelectrolyte multilayered-covered mesoporous TiO_2 nanoparticles was adsorbed on a QCM surface [12].

In this article, we aim to investigate the QCM positive frequency shift phenomenon that was also observed when the QCM sensitive layer was fabricated by using metal-organic frameworks (MOF) and a simple method to address such issue. During the last two decades, there has been a growing interest in the development of MOF for various purposes such as gas storage and adsorption processes since they are tailorable, highly porous and have high surface area [13,14]. Because of these properties, they are also suitable to be used as a sensitive layer of a QCM sensor where the change of mass will be induced by the adsorption and desorption process of certain molecules inside their porous structure [15–17]. However, since most of the MOFs are produced as nanoparticles, one of the major challenges in fabricating a robust MOF-based sensor lies in the effectiveness of turning them into a thin film that can oscillate synchronously with the QCM sensor. When this requirement is not fulfilled, the positive frequency shift phenomenon could also be observed in a MOF-based QCM sensor. We then propose that this effect could be simply eliminated by fabricating a composite consisting of the MOF nanoparticle and a polymer to increase bonding of MOF nanoparticles to the surface.

2. Materials and methods

2.1. Materials

Benzoic acid, zirconyl chloride octahydrate ($ZrOCl_2.8\ H_2O$) and zinc chloride ($ZnCl_2$) were purchased from Merck. Meso-tetra(4-carboxyphenyl)porphyrin (H_4TCPP) was purchased from BLD Pharmatech GmbH, Germany. Acetone, dimethylformamide (DMF) and hydrochloric acid 37 % were purchased from VWR. PEBAX polymer was kindly provided by Arkema GmbH (Düsseldorf, Deutschland).

2.2. Sensor preparation and performance evaluation

2.2.1. MOF-525(Zn) synthesis and characterization

In order to obtain MOF-525(Zn), a non-metalated MOF-525 was firstly synthesized by using benzoic acid as the modulator during the reaction following the previous procedure [18]. In a typical synthesis condition, 750 mg of $ZrOCl_2.8\ H_2O$ and 9 g of benzoic acid were firstly dissolved in a Pyrex vial containing 50 mL DMF by sonicating the suspension for about 10 min. Once a clear solution was obtained, the solution was then placed inside a convective oven and heated at 100^0 C for two hours. Afterwards, the solution was cooled down to room temperature and 250 mg of the porphyrin ligand (H_4TCPP) was then added and the solution was further sonicated for about 5 min to completely dissolve the ligand. The solution was then heated in a convective oven at 100^0 C for 24 h. Once the reaction finishes, the MOF-525 was collected by centrifugation (7000 rpm, 6 min) and washed with DMF and acetone. It has been reported that some ligated benzoates could still remain within the framework after the washing process [19]. Therefore, after the washing process, about 200 mg of MOF-525 was immersed in a mixture of 20 mL DMF and 1 mL of 8 M HCl in an oven at 100^0 C for 24 h. Afterwards, the product was cooled down to room temperature, centrifuged and washed with DMF and acetone. The MOF-525(Zn) was obtained by employing a post-metalation process on MOF-525. In a typical MOF-525 post-metalation process, 100 mg of MOF-525 was suspended in a 20 mL DMF containing 1.68 mmol of $ZnCl_2$. The suspension was then placed in a convective oven and heated at 100^0 C for 24 h. Once the reaction finishes, the product was filtered and washed with DMF and acetone.

The successfulness of the post-metalation process was then proven by observing the change of the UV-Vis spectra of the digested samples of MOF-525 and MOF-525(Zn). Both samples were firstly digested with 1 M NaOH and their UV-Vis spectra were recorded by using Cary 5000 UV/Vis Spectrophotometer equipped with Cary Universal Measurement Accessory (UMA). In addition, the crystallinity of the MOF-525(Zn) was also checked by collecting its powder X-Ray diffraction (PXRD) pattern using D8 A25 Da-Vinci Bruker XRD. The measurement took place between 2θ of $3–20^0$.

2.2.2. Fabrication of QCM sensor based on MOF-525(Zn) and MOF-525 (Zn)-PEBAX composite

All the sensors were prepared by using a 25 MHz QCM HC-49S sensor having a dimension around 8 × 2 mm. A closer look of this QCM sensor is given in the Fig. S1 in the Supplementary Information. For the MOF-525(Zn) sensor, the nanoparticle was firstly suspended in ethanol with concentration of 1 mg mL ^{1}. The suspension was then sonicated to obtain a homogeneous suspension. Afterwards, by using a plastic tube (diameter 1 mm), the suspension was drop-casted on top of the QCM sensor. The drop-casting process was repeated until the required amount of MOF film mass change was obtained. This was observed by continuously monitoring the frequency change of the QCM sensor during the drop-casting process.

Meanwhile, for the MOF-525(Zn) composite sensor, the MOF-525 (Zn) was firstly suspended inside a 2 wt% ethanolic PEBAX solution. The mass ratio between MOF-525(Zn) and PEBAX was controlled to be 1:1 and 9:1. As in the case of MOF-525(Zn), the suspension was then drop-casted on top of the QCM sensors and the process was repeated until the required amount of MOF-525(Zn)-PEBAX composite on the QCM sensor was obtained, which was also checked by continuously observing the frequency change of the QCM sensors. During the preparation of MOF-525(Zn) and MOF-525(Zn)-PEBAX composites, we attempted to keep the amount of materials on the QCM sensors to be identical by maintaining the frequency change of the QCM sensors to be around 9KHz.

2.2.3. Evaluation of the sensor performance

The performance of the MOF or MOF-composites sensors used in this study were evaluated by adsorption of four different analytes, namely xylene isomers (ortho-, meta- and para-xylene) and ethanol utilizing a 25 MHz QCM sensor array. The schematic diagram of the experimental setup is then given in Fig. 1. As illustrated in the schematic diagram, during the experiment, the vapor concentration of the xylene isomers or ethanol as the analyte was adjusted between 10 and 7000 ppm or between 10 and 4000 ppm, respectively, by controlling the flow rate of the analyte vapor and the nitrogen gas with mass flow controllers (MFC) that is used to dilute the analyte before it was introduced into the QCM array. In this study, controlling the analyte concentration introduced into the QCM array is crucial to observe the behavior of the QCM sensors at different analyte concentration.

The change of the QCM frequency shift was then continuously recorded during the experiment and presented here as the Δf ratio, which describes the normalized amount of the adsorbed analyte against the mass of the sensitive layer. This value is given by the equation:

$$\Delta f\ ratio(\%) = \frac{f \quad f_1}{f_0 \quad f_1} \times 100 \tag{2}$$

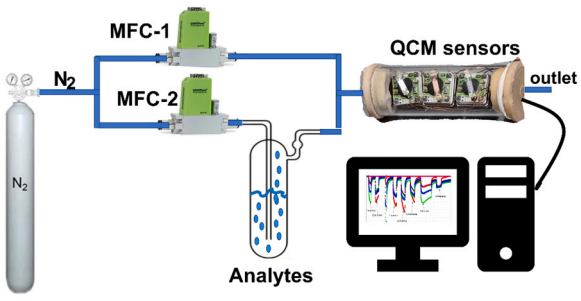

Fig. 1. The schematic diagram of the experimental setup.

where f_0 is the QCM frequency of an empty sensors, f_1 is the final QCM frequency after it was drop-casted with MOF nanoparticles or MOF composites and f is the measured QCM frequency after the adsorption of an analyte takes place.

3. Results and discussions

3.1. MOF-525(Zn)-based sensor performance to detect xylene isomers

Before assessing the performance of the sensors to adsorb various xylene isomers, we firstly characterized the MOF-525(Zn) nanoparticle. As has been previously stated, the MOF-525(Zn) was synthesized using a post-metalation method of MOF-525. The PXRD pattern of MOF-525 (Zn) and the calculated PXRD pattern for MOF-525 is then given in Fig. 2 (A). As can be seen, the PXRD pattern MOF-525(Zn) is identical with the calculated PXRD pattern of MOF-525. This is expected since the post-metalation process is not expected to change the topology of MOF-525 as its parent MOF. The success of MOF-525(Zn) fabrication is then proven by observing the transformation of the UV–vis spectra of the digested samples before and after the post-metalation process, as given in Fig. 2 (B). From the result, it can be seen that spectra of the digested MOF-525(Zn) is significantly different from MOF-525 and consistent with the previous result of post-metalation process of MOF-525 with Zn [20]. Therefore, it can be safely inferred that the MOF-525 has been successfully post-metalated to be MOF-525(Zn).

Having successfully synthesized the MOF-525(Zn), we attempted to use it as a sensitive layer material of a QCM sensor. In order to realize this, the ethanolic suspension of MOF-525(Zn) was drop-casted on a 25 MHz QCM sensor and then exposed to various xylene isomers at different concentrations, with the results are presented in Fig. 3.

From the result, it can be seen that the frequency shift of the QCM fabricated with MOF-525(Zn) as the sensitive layer when exposed to xylene isomers as the analyte goes to the positive direction rather than negative response. Higher QCM positive frequency shift is also observed as the analyte concentration of the xylene isomers is increased. These results then indicate that the Sauerbrey equation cannot be applied in the case when the MOF-525(Zn) is used as the sensitive layer of the QCM.

As previously stated, such a phenomenon is not peculiar to this case but has also been observed in other cases [4–8,10,12]. In 1985, Dybwad has predicted such a positive frequency by modelling the QCM as a pair of coupled oscillators [21,22], as illustrated in Fig. S2(A), which leads to the equation (S1). Johannsmann and Frank have also used a similar approach to yield an algebraically different but essentially identical equation from Dybwad's equation when they studied the capillary aging phenomenon of glass spheres upon contact with a QCM surface [23] and adsorption of micron-sized particle on a QCM surface [12]. In this case, they predict that a coupled oscillator model can be quantitively calculated based on the equation (S2). From both models, a discontinuity exists that divides the QCM frequency shift into two contrasting trends, as illustrated in Fig. S2(B), namely when $k = m\omega^2$ or when the ω is equal to $\omega_{particle}$, in which k, m and $\omega_{particle}$ are the elastic constant, mass and frequency of the particle attached to the QCM, respectively, and ω is the frequency of the QCM. Therefore, in the case where $\omega_{particle} >> \omega$, the frequency shift of a QCM is negative as predicted by Sauerbrey equation. Such a situation occurs where the particle is strongly attached unto the QCM surface so they can move synchronously together. In this scenario, the increase of contact stiffness between the particle and the QCM surface, namely k, will non-linearly decrease the QCM frequency change but its value will remain negative. In contrast, when $\omega >> \omega_{particle,}$ a positive frequency shift in the QCM is observed and the trend increases non-linearly with higher k value. This happens when the particle is loosely attached to the QCM surface.

Furthermore, the QCM positive frequency shift has also been explained by Hunt and co-workers by describing the phenomenon through the equation (S5) [24,25]. In this case, a positive frequency shift in the QCM can happen when the second term in the bracket of the equation, namely $\frac{\Delta\mu}{V_s^2}$, is dominant and gives a positive result, where $\Delta\mu$ and V_s are the change in the selective layer stiffness, and the acoustic wave velocity, respectively. From this equation, it can also be predicted that the QCM positive frequency shift will take place when the contact stiffness of the particle and the QCM surface increases, namely when $\mu_{perturbed}$ is greater than $\mu_{unperturbed}$.

From the above models, it could be inferred that the first and main requirement to obtain a QCM negative frequency shift is to strongly attach the sensitive layer on the QCM surface. When this condition is not fulfilled, the QCM frequency shift will be affected by the stiffness change of the selective layer. In the case of MOF-525(Zn) sensor, it could be firstly hypothesized that the sensitive layer stiffness of the MOF-525(Zn) increases in the presence of xylene isomers. Such an increase in stiffness could be mainly caused by the non-rigid or loose attachment between the MOF-525(Zn) and the QCM surface. As can be seen from the Fig. 4 (A), the top surface of the QCM is not fully covered by the MOF-525(Zn) nanoparticles, which is also corroborated by observing the QCM cross-section as presented in Fig. 4(B) that shows the absence of a homogeneous film. Therefore, it could be assumed that the drop-casted MOF-525(Zn) nanoparticles are rather being scattered as agglomerated nanoparticles on the QCM surface rather than forming a thin film. A further and closer inspection on the agglomerated nanoparticles on the QCM, as presented Fig. 4(C), also shows that, although the nanoparticles

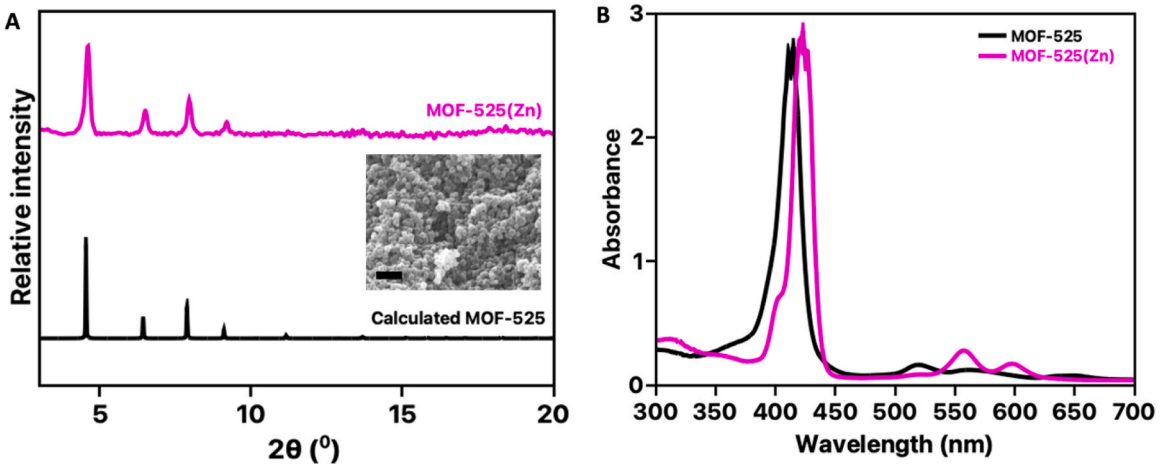

Fig. 2. The PXRD pattern of MOF-525(Zn) and the calculated pattern of MOF-525 (A) and the UV-Vis spectra of the digested samples of MOF-525 and MOF-525(Zn) (B). The micrograph of MOF-525(Zn) is given as an inset and the scalebar is 1 μm.

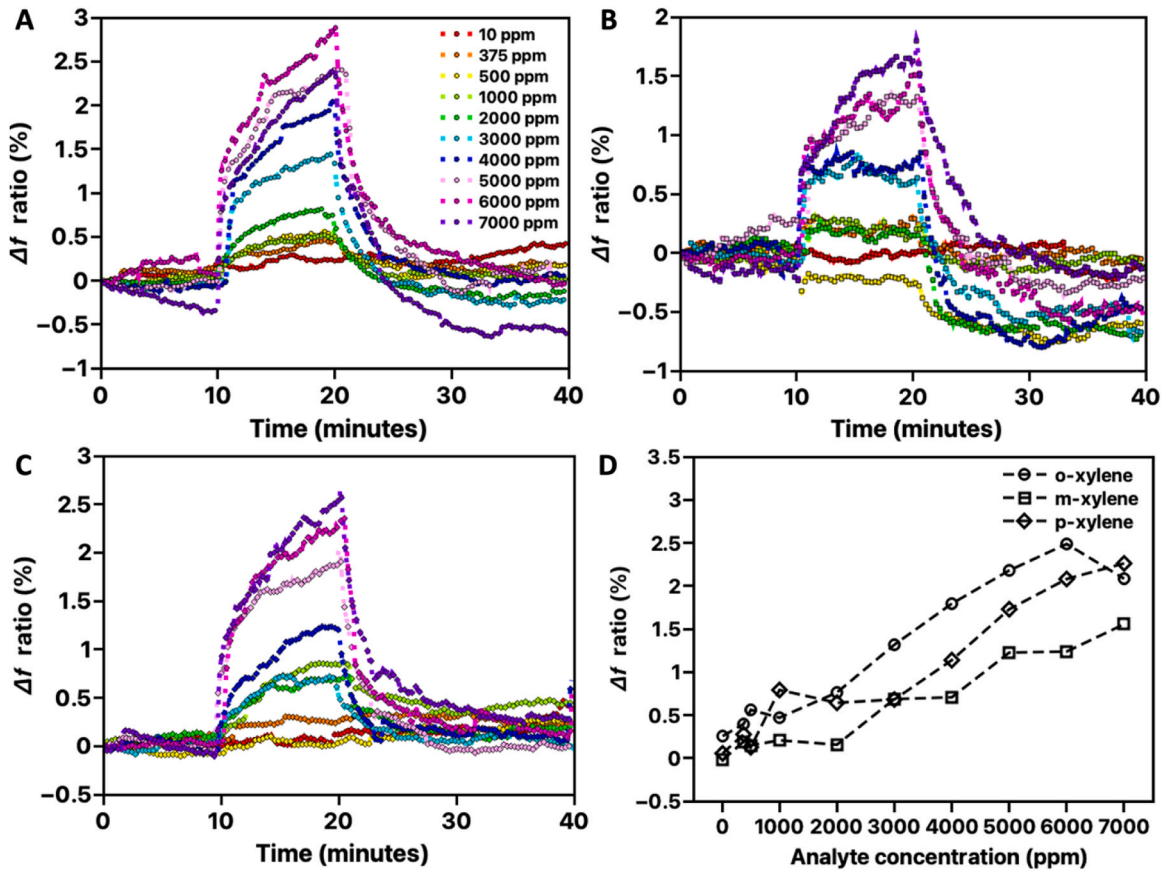

Fig. 3. The MOF-525(Zn) sensor performance to detect o-xylene (A), m-xylene (B), p-xylene (C) and the trend of the QCM frequency change against xylene isomers feed concentration (D).

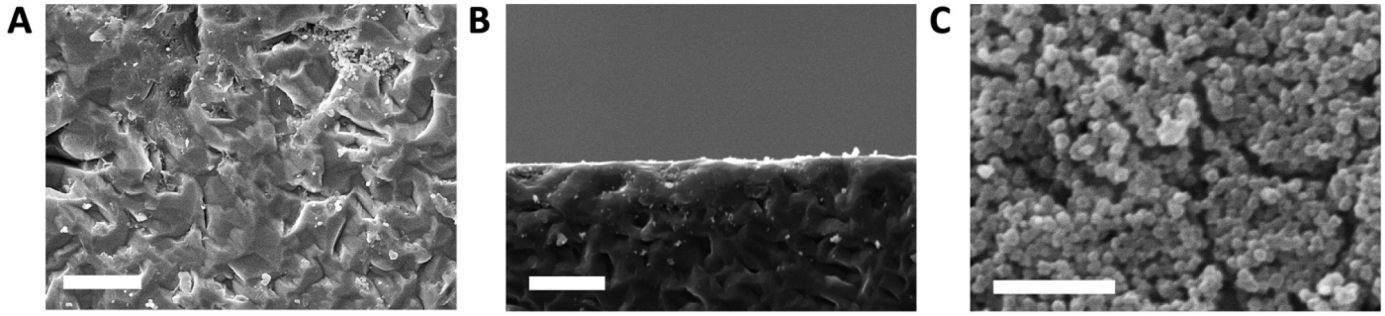

Fig. 4. The micrograph of the top surface (A), cross-section (B) and the agglomerated nanoparticles (C) of MOF-525(Zn) sensor. The scalebar is 5 μm, 10 μm and 20 μm, respectively.

are closely packed together, they are not closely attached to each other.

These conditions might contribute in MOF-525(Zn)-QCM surface bond loosening. It should be noted that, even though the negative QCM frequency shift was observed when the MOF-525(Zn) was firstly drop-casted on the QCM surface, this does not mean that the firstly established bond between the MOF-525(Zn) and the QCM surface cannot be disturbed or is strong enough to withstand perturbation when an analyte is introduced into the system. In this case, it could only be assumed that when the QCM surface was initially drop-casted with MOF-525(Zn), the resonance frequency of the MOF-525(Zn) ($\omega_{particle}$) is greater than the resonance frequency of the QCM so that the first term in the bracket of the equation (S5) is more dominant than the second term resulting in a synchronous oscillation of the MOF-525(Zn) sensor.

However, once the xylene isomers were fed into the system, the initially established bond between the MOF-525(Zn) and QCM surface might be disturbed. Such a disturbance might come from two possibilities. The first possibility could be contributed from the intrusion of the xylene isomers at the interface of MOF-525(Zn) and the QCM surface. In this case, the xylene isomers might loosen the initial bonding between the MOF-525(Zn) and the QCM surface resulting in a looser attachment of the MOF-525(Zn) to the QCM surface in comparison to the initial case. Secondly, it might also be the case that the MOF-525(Zn) interacts strongly with the xylene isomers so that such an interaction disturb and loosen the initial bonding between the MOF-525(Zn) and QCM surface. Such a case could be similar with the case when a QCM positive frequency shift is observed when an antibody experiences a conformational change upon the adsorption of its specific target [25]. Both cases could lead to the reduction of the MOF-525(Zn) resonance frequency ($\omega_{particle}$ in equation (S2) and (S4)). Consequently, in comparison to the initial condition, the $\omega_{particle}$ is now lesser than the QCM resonance frequency

so that the operating regime of the MOF-525(Zn) QCM sensor is now changed from the inertial to elastic loading region where a positive frequency shift is observed and its value is affected by the stiffness of the sensitive layer [12]. In this case, the second term in the bracket of the equation (S5) also becomes more dominant than the first term.

Since the MOF-525(Zn) sensor now operates in the elastic loading regime, the frequency shift will also be affected by the stiffness of the sensitive layer, namely higher positive frequency shift is expected with increasing stiffness. This is then reflected when one looks at the result as presented Fig. 3 (D). It can be seen from the result that the QCM frequency shift becomes more positive as the xylene isomers concentration increases. This could clearly indicate that, as the xylene isomers concentration gets higher, the stiffness of the sensitive layer also increases. In this case, the xylene isomers might act as a bridge that intensifies the contact between the already-loosened-MOF-525(Zn) and QCM surface [23]. Therefore, the higher the xylene isomers concentration, the more bridges will be established between the already-loosened-MOF-525(Zn) and QCM surface. This condition will then result in a higher-pressure condition experienced by the QCM. Consequently, the k and $\Delta\mu$ value in the equation (S1) and (S5), respectively, also gets higher when more xylene isomers are introduced into the system, which is then clearly reflected by the more positive QCM frequency shift at higher xylene isomers concentration.

This result has also been corroborated when we attempted to fabricate a MOF-525(Zn) sensor by employing a 5 MHz gold QCM with the results are presented in the Fig. S3 (A-C) in the Supplementary Information. In contrast to the trend obtained in the 25 MHz QCM sensor, the MOF-525(Zn) on the 5 MHz gold QCM sensor exhibits a negative frequency shift. Moreover, it can also be observed that higher analyte concentration analyte also leads to a more negative QCM frequency shift before it reaches the plateau that indicates the saturation of the adsorption capacity. There are then two plausible explanations in this case that could be related with the previous phenomenon of the positive frequency shift. First, as the QCM frequency used in this particular case is significantly lower than the previous one, the $\omega_{particle}$ of the MOF-525 (Zn) could be higher than the ω of the QCM. Second, the attachment of the MOF-525(Zn) nanoparticles on the gold QCM surface in this particular case is better than the case of the silver 25 MHz QCM. Both conditions then fulfill the requirement for the QCM to operate in the inertial loading region resulting in a QCM negative frequency as predicted in the Sauerbrey equation.

Since the loosening bond between the MOF-525(Zn) and the QCM surface might be the major cause of the QCM positive frequency shift in the previous case, the main strategy to reverse the trend is to strengthen such bonding so that the $\omega_{particle}$ is always higher than the ω, even when the xylene isomers concentration in the system is increased, in order to ensure the harmonious oscillation of the sensor. To address the above challenge, we attempted to fabricate a composite sensor that was based on the MOF-525(Zn) and a polymer. In this case, we chose PEBAX as the polymer because of its rubbery nature. We hypothesized that the rubbery nature of PEBAX could be beneficial since it could act as a glue to provide a stronger attachment between the MOF-525(Zn) and the QCM surface. The first composite sensor was then fabricated by mixing MOF-525(Zn) and PEBAX in a weight ratio of 9:1 and the performance result of this sensor towards all the xylene isomers is given in Fig. 5.

As presented in the result, it can now be seen that not all the experiment conditions result in a QCM positive frequency shift. When the feed concentration of the xylene isomers is below 1000 ppm, the reduction in the QCM frequency can be observed. This means that the composite sensor now operates in the region of inertial loading instead of elastic loading [12]. This trend, however, starts to reverse when the xylene isomers concentration is increased above 1000 ppm. As can be

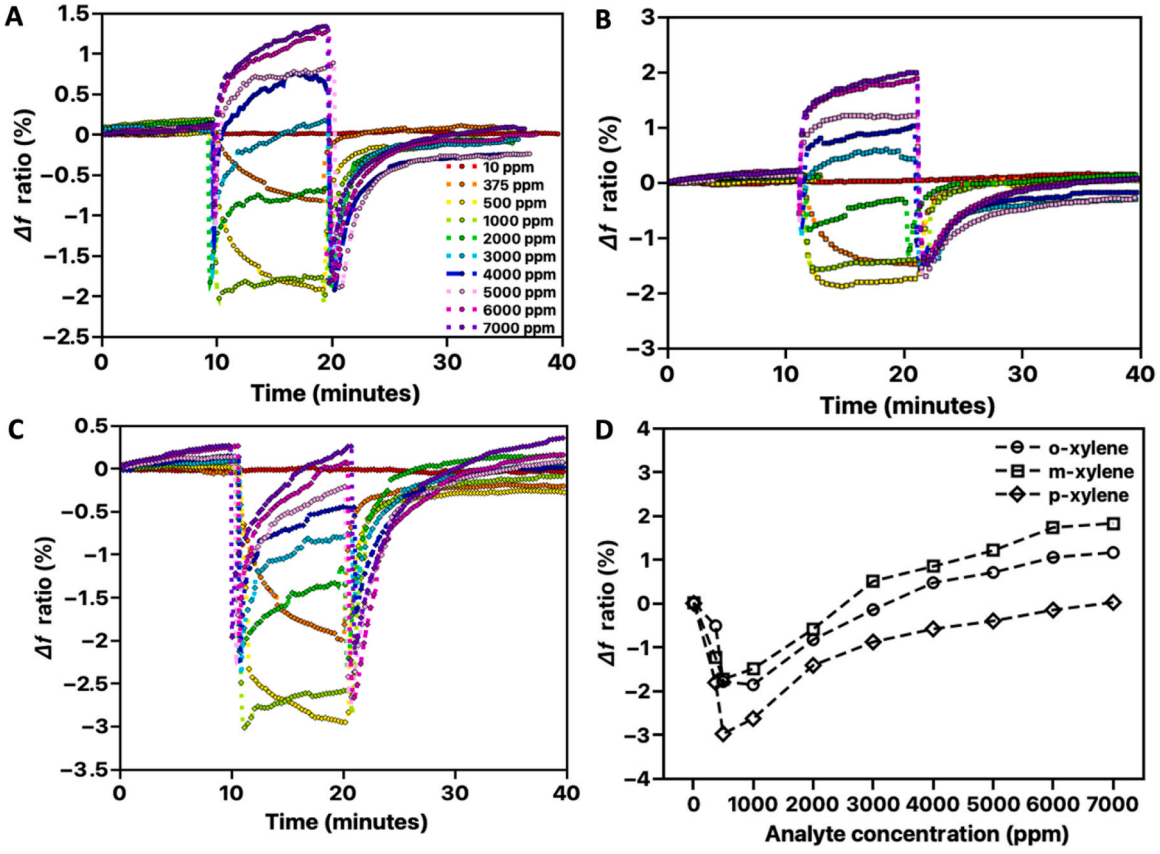

Fig. 5. The MOF-525(Zn)-PEBAX (9:1) composite sensor performance to detect o-xylene (A), m-xylene (B), p-xylene (C) and the trend of the QCM frequency change against xylene isomers feed concentration (D).

seen, the reduction in the QCM frequency firstly takes place in the first few seconds after the introduction of the xylene isomers. Afterwards, during the stabilization period, the QCM frequency quickly returns back to the positive direction. Interestingly, the positive frequency shift of the composite sensor can also spontaneously return back to the negative direction at the beginning of the cleaning period before finally reaching the initial baseline. When the trend of the QCM frequency shift is plotted against the feed concentration of the xylene isomers, as presented in Fig. 5 (D), it can be clearly observed that a critical analyte concentration does exist where the QCM frequency shift is reversed from negative to positive.

From these results, the positive impact of having polymer as an additional material for the sensor to reverse the QCM frequency shift is obvious, although the impact is still limited. In this case, it could be firstly hypothesized that at low xylene isomers concentration (below 1000 ppm), the $\omega_{particle}$ is always higher than the ω, including when the xylene isomers are in the system. During this period, the interaction bond between MOF-525(Zn) and the QCM surface is not significantly disturbed, which might be contributed from the polymer that acts as a glue to make a stronger attachment between the MOF-525(Zn) and the QCM surface. This could then be seen from the micrograph of the surface of the MOF-525(Zn)-PEBAX (9:1) composite sensor as presented in Fig. 6 (A). Although some scattered agglomerated nanoparticles can still be seen on the QCM top surface, its top surface is relatively smoother than the top surface of MOF-525(Zn) sensor, which might indicate the existence of a PEBAX polymer on the QCM surface.

Despite this, as presented in Fig. 6 (B), the existence of a homogeneous film cannot still be clearly seen through the cross-section of the MOF-525(Zn)-PEBAX (9:1) composite sensor. In addition, the physical appearance of the agglomerated nanoparticles of the MOF-525(Zn)-PEBAX (9:1) composite sensor, as presented in Fig. 6 (C), also does not show any significance difference in comparison to the MOF-525(Zn) sensor. Such a condition might then contribute to the QCM positive frequency shift phenomenon that is observed when the xylene isomers concentration is increased above 1000 ppm. In this case, even though the bond interaction between the MOF-525(Zn) and the QCM surface in the MOF-525(Zn)-PEBAX (9:1) composite sensor is stronger than in the case of MOF-525(Zn) sensor, such a bond could still be disturbed at higher xylene isomers concentration. Moreover, it could also be the case that some MOF-525(Zn) nanoparticles might not be bonded with PEBAX to the QCM surface. The bonding of these loose MOF-525(Zn) nanoparticles and the QCM surface might be disturbed at the beginning when the analyte is introduced but its impact might still be masked by the dominance from first term in the equation (S5). When the analyte concentration is further increased, its impact is more pronounced and now the second term in equation (S5) starts to dominate the trend of the QCM frequency shift.

As in the case in MOF-525(Zn) sensor, these conditions could lead to the increase of the sensitive layer stiffness as the xylene isomers concentration in the system becomes higher. In this case, when the concentration of the xylene isomers is elevated above 1000 ppm, the $\omega_{particle}$ starts to become lower than the ω. As a consequence, the MOF-525(Zn)-PEBAX (9:1) composite sensor now operates in the elastic loading region where the QCM frequency shift is affected by the stiffness of the sensitive layer. This is clearly indicated in the result showing that as the xylene isomers concentration is increased above 1000 ppm, the QCM positive frequency shift also becomes higher because of the sensitive layer stiffness increase. Despite this, it can also be seen that, in comparison to the MOF-525(Zn) sensor, the increase in the QCM positive frequency in MOF-525(Zn)-PEBAX (9:1) composite sensor is slower and shows a plateauing tendency. This might suggest that the impact of the stiffness increase in MOF-525(Zn)-PEBAX (9:1) composite sensor is more limited than in MOF-525(Zn) sensor because of the strengthening contribution that comes from the polymer.

Afterwards, when the xylene isomers were swept out from the system, it can also be seen from the result that the QCM positive frequency shift quickly goes to the negative direction before reaching the initial condition. This then happens because, as the xylene isomers concentration in the system is greatly reduced, the sensitive layer stiffness of the MOF-525(Zn)-PEBAX (9:1) composite sensor is also reduced and thus reducing the amplitude of the QCM positive frequency shift. More importantly, it should also be noted that the frequency shift is not only reduced in regards to its amplitude, but also goes to the negative direction, suggesting that the $\omega_{particle}$ is now higher than the ω. Therefore, as the xylene isomers are removed from the system, the initially strong interaction between the MOF-525(Zn)-PEBAX(9:1) composite and the QCM surface is brought back and the composite sensor now oscillates harmoniously.

This preliminary result shows that employing PEBAX as an additional material in the sensitive layer of a MOF-based QCM could help to address the issue of the QCM positive frequency shift. However, the amount of this polymer has to be significant enough to maintain higher $\omega_{particle}$ than the ω so that the QCM frequency shift always goes to the negative direction. Therefore, a new composite sensor was fabricated with higher polymer content by adjusting the ratio between the MOF and polymer to be equal. The performance result of the MOF-525(Zn)-PEBAX (1:1) composite sensor to detect xylene isomers is presented in Fig. 7.

As can be seen in the results, the positive frequency shift as previously observed in both MOF-525(Zn) and MOF-525(Zn)-PEBAX (9:1) composites sensor has been completely eliminated. In this case, the composite sensor gives a negative frequency change as expected in a normal QCM situation. Therefore, in this case, $\omega_{particle}$ is always significantly higher than the ω regardless of the concentration of the xylene isomers in the system resulting in a composite sensor that operates in the inertial loading region rather than in the elastic loading one.

The microstructure of the MOF-525(Zn)-PEBAX (1:1) composites sensor was then investigated and the results are presented in Fig. 8. Firstly, as can be seen in Fig. 8 (A), the top surface of the MOF-525(Zn)-PEBAX (1:1) composites sensor is relatively smoother than the MOF-525

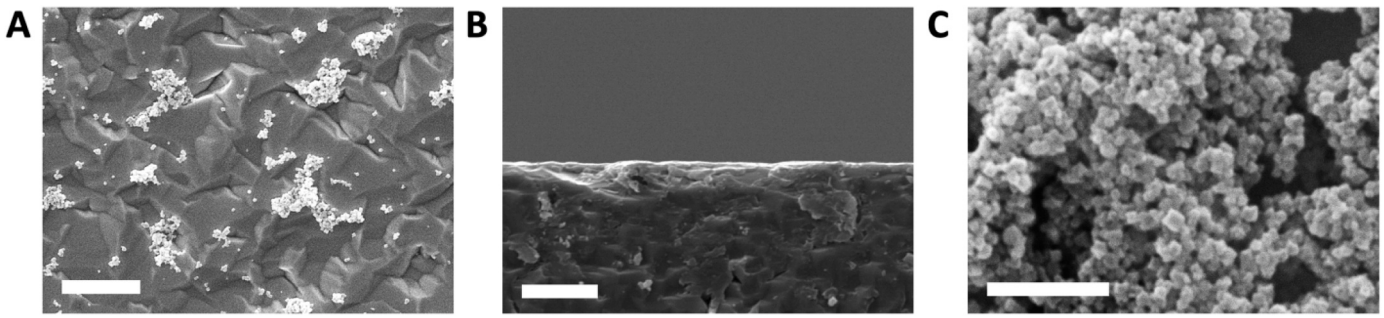

Fig. 6. The micrograph of the top surface (A), cross-section (B) and the agglomerated nanoparticles (C) of MOF-525(Zn)-PEBAX (9:1) composite sensor. The scalebar is 5 μm, 10 μm and 20 μm, respectively.

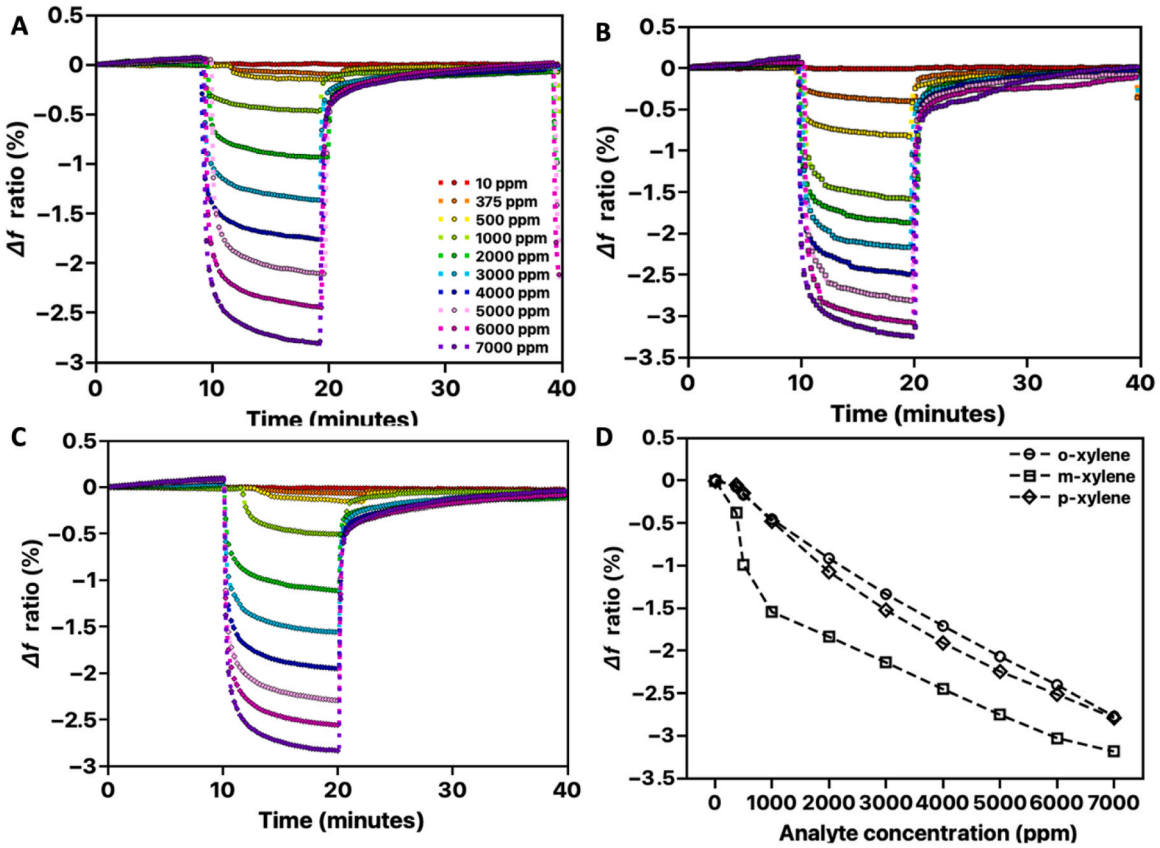

Fig. 7. The MOF-525(Zn)-PEBAX (1:1) composite sensor performance to detect o-xylene (A), m-xylene (B), p-xylene (C) and the trend of the QCM frequency change against xylene isomers feed concentration (D).

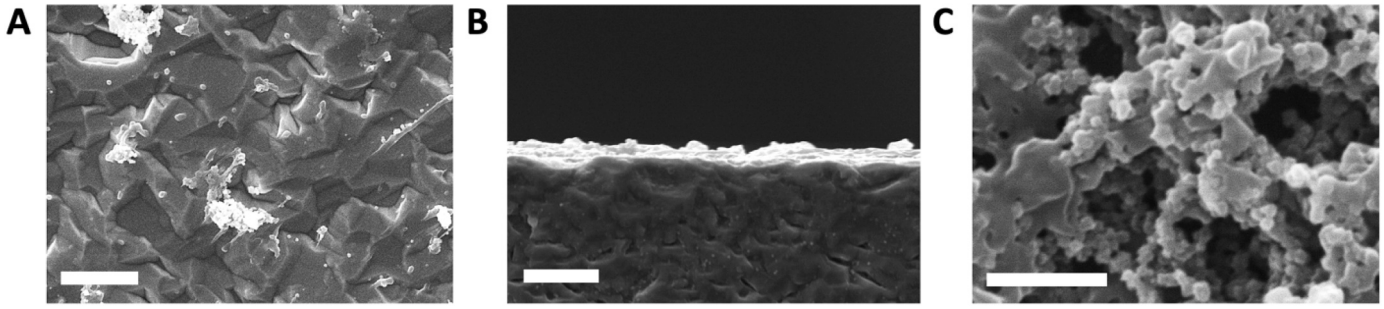

Fig. 8. The micrograph of the top surface (A), cross-section (B) and the agglomerated nanoparticles (C) of MOF-525(Zn)-PEBAX (1:1) composite sensor. The scalebar is 5 μm, 10 μm and 20 μm, respectively.

(Zn) sensor. However, the appearance of the top surface of this sensor might not be clearly different if compared with the MOF-525(Zn)-PEBAX (9:1) composites sensor. Despite this, a contrasting situation can be seen upon closer inspection on the cross-section of the MOF-525 (Zn)-PEBAX (1:1) composites sensor. As can be seen in Fig. 8(B), the formation of a thin film can now be seen in the MOF-525(Zn)-PEBAX (1:1) composite sensor. This then shows the contribution of the PEBAX polymer in forming a homogeneous layer on the surface of the QCM surface. Furthermore, the PEBAX polymer also contribute in affecting the physical property of the MOF-525(Zn) nanoparticles. As can be seen in Fig. 8(C), the physical appearance of the agglomerated MOF-525(Zn) nanoparticles are significantly different with the previous two cases. In this case, it can be seen that the PEBAX polymer starts to envelope the nanoparticles and bind them together.

Having observed the performance and the micrograph of the MOF-525(Zn)-PEBAX (1:1) composite sensor, it could be safely inferred that employing the PEBAX polymer as an additional component to form a composite sensor is beneficial in eliminating the positive frequency shift in the QCM sensor. The PEBAX has two important roles. Firstly, the use of PEBAX is crucial in forming a thin and homogeneous layer that cannot otherwise be achieved when the QCM sensor was only fabricated using MOF-525(Zn) nanoparticles. In this case, the PEBAX will also act as a glue between the MOF-525(Zn) and the top surface of the QCM sensor to strengthen their interaction bonding. Secondly, the PEBAX polymer also contributes in binding the MOF-525(Zn) nanoparticles together. This will ensure that the agglomerated particle in the composite sensor could also oscillate harmoniously without slip. Since the MOF-525(Zn)-PEBAX (1:1) sensitive layer is now attached strongly on the QCM surface, the presence of xylene isomers in the system will not disturb this attachment. Therefore, $\omega_{particle}$ is always significantly higher than the ω and the QCM positive frequency shift can be completely eliminated.

However, although the positive impact of fabricating a composite

sensor by mixing PEBAX polymer with the MOF-525(Zn) nanoparticle in eliminating the positive frequency shift in the QCM sensor has been proven to be effective, it should also be noted that the PEBAX contribution in adsorbing the xylene isomers cannot be fully neglected. As given in the Fig. S4 in the Supporting Information, a QCM that was fabricated with only PEBAX as the sensitive layer has also shown the capability of the PEBAX polymer to adsorb the xylene isomers. For example, for the case of the highest xylene isomer concentration, the Δf ratio in the pure PEBAX QCM sensor for ortho-, meta-, and para xylene isomers is found to be around 1.88, 2.53 and 2.34, respectively. As also previously observed with polymeric materials as an affinity layer in a QCM, this might be caused by the polymer that can also act as a matrix that has the ability to adsorb and engulf the analyte within its structure [26]. However, this does not mean that the amount of the xylene isomers adsorbed in the MOF-525(Zn)-PEBAX (1:1) composite sensor is only contributed from the PEBAX. This is because the QCM frequency change in the MOF-525(Zn)-PEBAX (1:1) composite sensor is higher in comparison to the PEBAX sensor. At the same xylene feed concentration, the change of the normalized frequency of MOF-525 (Zn)-PEBAX (1:1) composite sensor is found to be around 2.77, 3.18, and 2.79, respectively, and thus corresponding to an increase of around 47 %, 26 % and 20 %, respectively. Although it could be argued that such an increase is not as big as expected, it could still be safely inferred that the presence of PEBAX does not completely block the MOF-525(Zn) pores so they can still contribute in adsorbing xylene isomers. Moreover, it could also be the case that the sensitivity of MOF-525(Zn) towards xylene isomers is not particularly high that could result in a tremendous change in the Δf ratio in comparison with the PEBAX QCM sensor. This conclusion can be more obvious when we tried to generalize this technique with other MOFs, namely MOF-525 and NU-902, to detect ethanol as will be further discussed below.

3.2. Generalizability of the approach

In order to investigate the possibility to generalize this strategy to other systems, we then studied three different sensors whose sensitive layer is fabricated by using MOF-525, MOF-525(Zn) and NU-902 to detect ethanol. MOF-525 is the non-metalated version of MOF-525(Zn). Meanwhile, NU-902 is another porphyrin-based MOF that was synthesized using the same starting material of MOF-525 albeit the reaction was carried out by using different modulator (4-methoxybenzoic acid instead of benzoic acid) and conducted at lower temperature (80^0 C instead of 100^0 C) [27,28]. The purity of both nanoparticles is proven through the matching PXRD pattern between the as-synthesized and the calculated pattern, as given in the Fig. S5 in the Supporting Information. During the study, the ethanol concentration was varied between 125 and 4000 ppm. The performance of the sensors that were purely fabricated with MOFs nanoparticles as the sensitive layer was firstly investigated and the result is presented in Fig. 9.

As expected, all the sensors exhibit the enhancement instead of the reduction of the crystal frequency. This clearly indicates the deviation from the Sauerbrey behavior, which could be again attributed to the poor attachment of the MOF nanoparticles on the QCM surface. In this case, as the ethanol is introduced into the system, the interaction bond between the MOF nanoparticles and the QCM top surface starts to be disturbed, resulting in lower $\omega_{particle}$ than ω. With increasing ethanol concentration, the stiffness of the already-loosened-bonding between the MOF nanoparticles and QCM top surface increases and thus resulting in higher QCM positive frequency shift. However, it can also be seen that when the ethanol concentration is further increased above 1000 ppm,

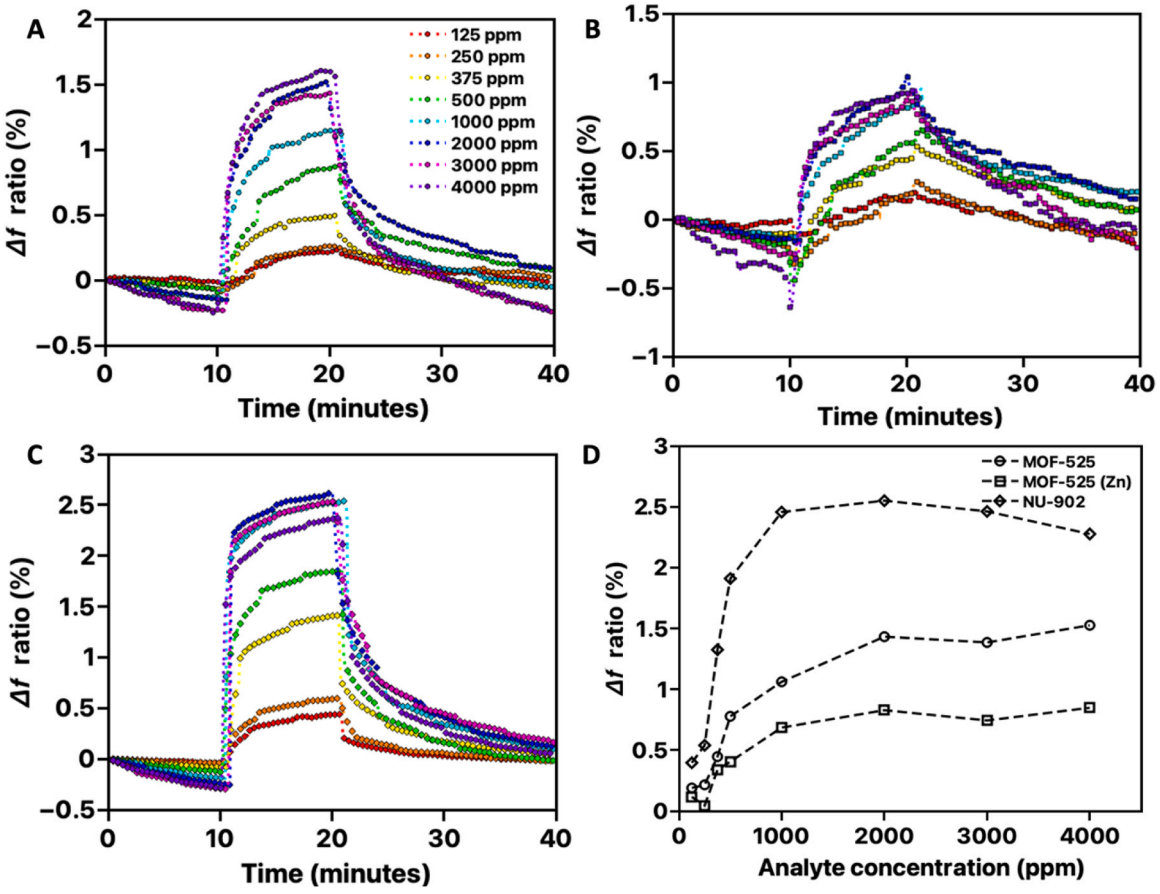

Fig. 9. The QCM sensor performance fabricated using MOF-525 (A), MOF-525(Zn) (B) and NU-902 (C) as the sensitive layer to detect ethanol and their trend of QCM frequency change against ethanol feed concentration (D).

the Δf ratio seems to be plateauing. In this case, it could be hypothesized that the stiffness of the loosened sensitive layer could no longer be increased with higher analyte concentration. Despite this, since the $\omega_{particle}$ is already lower than ω, the QCM frequency shift still moves to the positive direction. The same strategy was then applied to eliminate the QCM positive frequency shift, namely by fabricating a composite sensor consisting of the MOF and PEBAX polymer with equal weight ratio and the performance of the composite sensors is given in Fig. 10.

As can be seen from the result, all the composite sensors now experience the reduction of the crystal frequency and an almost linear relationship can be established between the Δf ratio and ethanol feed concentration. In this case, $\omega_{particle}$ is always higher than the ω because of the strong attachment of the MOF-PEBAX (1:1) sensitive layer on top of the QCM surface. Such a strong attachment cannot be deformed even when the ethanol is present in the system resulting in a consistent QCM negative frequency shift for the whole range of ethanol concentration. However, as in the case with the xylene isomers, the pure PEBAX QCM sensor also shows some adsorption towards ethanol (Fig. S6 in the Supporting Information). In the case of 4000 ppm ethanol, for example, the Δf ratio of the pure PEBAX sensor is found to be around 0.13. Despite this, at the same concentration, the Δf ratio for MOF-525-, MOF-525(Zn)-, and NU-902-PEBAX (1:1) composite sensor is found to be around 0.24, 0.48 and 0.28, respectively, which corresponds to an increase of the Δf ratio around 85 %, 269 % and 115 %, respectively. In comparison to the previous case with xylene isomers, the difference of ethanol uptake between the composite sensor and the pure PEBAX sensor is more obvious. This could be caused by the fact that these MOFs are quite sensitive to ethanol as previously reported [29]. Furthermore, this also strengthens our previous hypothesis that the pores of the MOFs are not completely blocked by the polymer so that the MOFs can still contribute in the adsorption process.

The summary of the QCM positive frequency shift phenomena and its elimination strategy in both MOF and MOF composite sensor is then given in Fig. 11. As can be seen from the illustration, in the beginning, both the MOF nanoparticles and the QCM can oscillate harmoniously since in this case the $\omega_{particle}$ is always higher than the ω and thus resulting in a QCM negative frequency shift. However, as analytes are introduced into the system, the MOF sensor experiences disturbance on its bonding with the QCM surface. As a consequent, the operating regime of the MOF sensor now changes from inertial to elastic loading regime where $\omega_{particle}$ is now lower than ω and the QCM positive frequency shift is observed. This also means that the QCM frequency shift will now also be affected by the sensitive layer stiffness, namely higher stiffness leads to higher positive frequency. Such a situation, however, does not occur in both MOF-composite sensors since the presence of the analytes is not significant enough to initiate a disturbance on the attachment between the MOF nanoparticles and the QCM surface. When the analyte concentration is further increased, the stiffness of the sensitive layer of the MOF sensor further increases because of the accumulation of the analytes at the interface of MOF and the QCM surface or because of the rearrangement of the MOF nanoparticles on the QCM surface and thus resulting in a higher QCM positive frequency shift. The same positive frequency effect is also experienced by MOF-PEBAX (9:1) composite sensor since now the analyte concentration in the system is high enough to disturb the attachment of the sensitive layer and the QCM surface, although its impact is not as great as in the case of MOF sensor. Lastly, only the MOF-composite sensor with sufficient amount of polymer, MOF-PEBAX (1:1) in this case, can give the QCM negative frequency across the whole range of the analyte concentrations and eliminate the QCM positive frequency shift phenomenon because of the strong

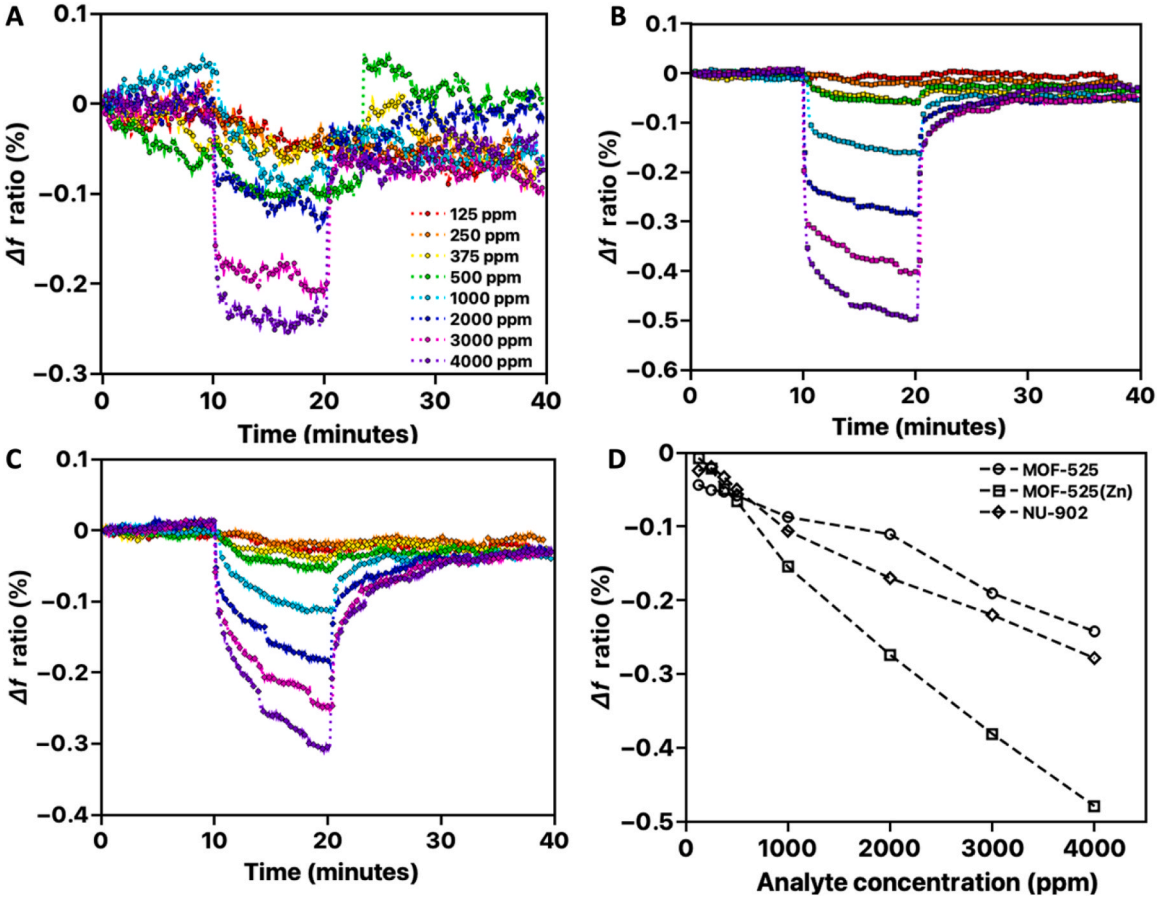

Fig. 10. The QCM composite sensor performance fabricated using MOF-525-PEBAX (1:1) (A), MOF-525(Zn)-PEBAX (1:1) (B) and NU-902-PEBAX (1:1) (C) as the sensitive layer to detect ethanol and their trend of QCM frequency change against ethanol feed concentration (D).

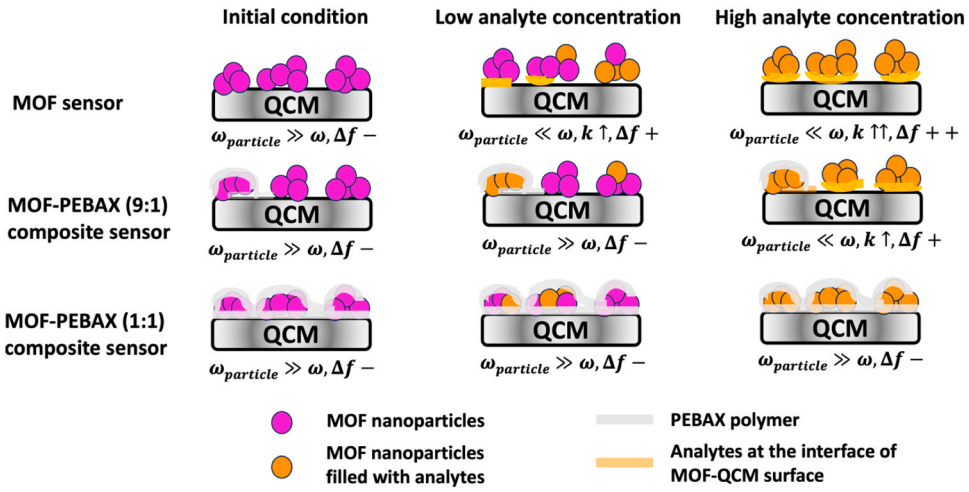

Fig. 11. The illustration of the QCM positive frequency shift phenomenon and its elimination strategy in MOF and MOF composite QCM sensor.

attachment between the sensitive layer and the QCM surface.

4. Conclusions

In conclusion, we have successfully shown in this study that the QCM positive frequency shift observed in the MOF-based sensor can actually be reversed by using a simple strategy, namely by fabricating a composite sensor. In the absence of the polymer, the MOF nanoparticles cannot form a homogeneous thin film on top of the CM surface and a strong interaction bonding between the MOF and the QCM surface cannot be established. In the presence of an analyte, this bonding will be disturbed resulting in lower $\omega_{particle}$ than ω. Consequently, the MOF-based QCM operates in the elastic loading region where the stiffness increases between the MOF nanoparticles as the sensitive layer and the QCM surface, which happens at higher analyte concentration, leads to higher QCM positive frequency shift. When a polymer is introduced to fabricate a composite sensor, such a perturbation in the bonding could be minimized because the polymer acts as a glue to strengthen this bonding. As a result, the MOF composite QCM sensor can now operate in the inertial loading region where negative frequency shift can be observed. However, a sufficient amount of polymer must be used to fabricate the composite sensor because otherwise the $\omega_{particle}$ cannot be maintained to be always higher than the ω and the QCM will back operate in the elastic loading region. In our case, we observe that fabricating a composite sensor comprising of porphyrin-base MOFs and PEBAX with 1:1 wt ratio gives satisfactory results to reverse the QCM positive frequency shift trend that is observed in the non-composite MOF-based sensor. This strategy might then be translated to other MOF-based systems where QCM positive frequency shift occurs caused by the weak attachment between the MOF nanoparticles and the QCM surface.

CRediT authorship contribution statement

Nicholaus Prasetya: Conceptualization, Methodology, Validation, Formal analysis, Investigation, Resources, Writing – original draft, Writing – review & editing, Visualization, Supervision, Project administration, Funding acquisition. **Salih Okur:** Conceptualization, Methodology, Software, Validation, Formal analysis, Investigation, Resources, Data curation, Visualization, Supervision, Project administration, Writing - review & editing.

Declaration of Competing Interest

The authors declare that they have no known competing financial interests or personal relationships that could have appeared to influence the work reported in this paper.

Data availability

Data will be made available on request.

Acknowledgements

N. P acknowledges the funding from the Alexander von Humboldt Postdoctoral Fellowship (Ref 3.3 – GBR – 1219268 – HFST-P). S.O acknowledges the support from Helmholtz Funding Program Oriented Research IV, Key Technology Program 43 Program Material Systems Engineering (MSE). The authors also acknowledge the kind support from Dr Simon Ludwanowski from Arkema for providing the PEBAX polymer.

References

[1] F.N. Dultsev, E.A. Kolosovsky, QCM model as a system of two elastically bound weights, Sens. Actuators B Chem. 242 (2017) 965–968.
[2] U. Latif, S. Can, O. Hayden, P. Grillberger, F.L. Dickert, Sauerbrey and anti-Sauerbrey behavioral studies in QCM sensors—detection of bioanalytes, Sens. Actuators B Chem. 176 (2013) 825–830.
[3] S. Kravchenko, B. Snopok, "Vanishing mass" in the Sauerbrey world: quartz crystal microbalance study of self-assembled monolayers based on a tripod-branched structure with tuneable molecular flexibility, Analyst 145 (2020) 656–666.
[4] N. Üzar, S. Okur, M.Ç. Arıkan, Investigation of humidity sensing properties of ZnS nanowires synthesized by vapor liquid solid (VLS) technique, Sens. Actuators A Phys. 167 (2011) 188–193.
[5] T. Ates, C. Tatar, F. Yakuphanoglu, Preparation of semiconductor ZnO powders by sol–gel method: humidity sensors, Sens. Actuators A Phys. 190 (2013) 153–160.
[6] A. Erol, S. Okur, B. Comba, Ö. Mermer, M. Arıkan, Humidity sensing properties of ZnO nanoparticles synthesized by sol–gel process, Sens. Actuators B Chem. 145 (2010) 174–180.
[7] A. Erol, S. Okur, N. Yağmurcukardeş, M.Ç. Arıkan, Humidity-sensing properties of a ZnO nanowire film as measured with a QCM, Sens. Actuators B Chem. 152 (2011) 115–120.
[8] S. Okur, N. Üzar, N. Tekgüzel, A. Erol, M.Ç. Arıkan, Synthesis and humidity sensing analysis of ZnS nanowires, Phys. E Low Dimens. Syst. Nanostruct. 44 (2012) 1103–1107.
[9] L. Wang, J. Xu, X. Wang, Z. Cheng, J. Xu, Facile preparation of N-rich functional polymer with porous framework as QCM sensing material for rapid humidity detection, Sens. Actuators B Chem. 288 (2019) 289–297.
[10] H. Tai, Y. Zhen, C. Liu, Z. Ye, G. Xie, X. Du, Y. Jiang, Facile development of high performance QCM humidity sensor based on protonated polyethylenimine-graphene oxide nanocomposite thin film, Sens. Actuators B Chem. 230 (2016) 501–509.

[11] M. Yang, J. He, X. Hu, C. Yan, Z. Cheng, CuO nanostructures as quartz crystal microbalance sensing layers for detection of trace hydrogen cyanide gas, Environ. Sci. Technol. 45 (2011) 6088–6094.
[12] A. Pomorska, D. Shchukin, R. Hammond, M.A. Cooper, G. Grundmeier, D. Johannsmann, Positive frequency shifts observed upon adsorbing micron-sized solid objects to a quartz crystal microbalance from the liquid phase, Anal. Chem. 82 (2010) 2237–2242.
[13] T. Jia, Y. Gu, F. Li, Progress and potential of metal-organic frameworks (MOFs) for gas storage and separation: a review, J. Environ. Chem. Eng. (2022), 108300.
[14] N. Prasetya, I.G. Wenten, M. Franzreb, C. Wöll, Metal-organic frameworks for the adsorptive removal of pharmaceutically active compounds (PhACs): comparison to activated carbon, Coord. Chem. Rev. 475 (2023), 214877.
[15] K.N. Chappanda, O. Shekhah, O. Yassine, S.P. Patole, M. Eddaoudi, K.N. Salama, The quest for highly sensitive QCM humidity sensors: the coating of CNT/MOF composite sensing films as case study, Sens. and Actuators B Chem. 257 (2018) 609–619.
[16] P. Qin, B.A. Day, S. Okur, C. Li, A. Chandresh, C.E. Wilmer, L. Heinke, VOC mixture sensing with a MOF film sensor array: detection and discrimination of Xylene Isomers and their Ternary Blends, ACS Sens. 7 (2022) 1666–1675.
[17] M.A. Andrés, M.T. Vijjapu, S.G. Surya, O. Shekhah, K.N. Salama, C. Serre, M. Eddaoudi, O. Roubeau, I. Gascón, Methanol and humidity capacitive sensors based on thin films of MOF nanoparticles, ACS Appl. Mater. Interfaces 12 (2020) 4155–4162.
[18] K. Yu, I. Ahmed, D.-I. Won, W.I. Lee, W.-S. Ahn, Highly efficient adsorptive removal of sulfamethoxazole from aqueous solutions by porphyrinic MOF-525 and MOF-545, Chemosphere 250 (2020), 126133.
[19] P. Deria, D.A. Gómez-Gualdrón, I. Hod, R.Q. Snurr, J.T. Hupp, O.K. Farha, Framework-topology-dependent catalytic activity of zirconium-based (porphinato) zinc (II) MOFs, J. Am. Chem. Soc. 138 (2016) 14449–14457.
[20] C.-W. Kung, T.-H. Chang, L.-Y. Chou, J.T. Hupp, O.K. Farha, K.-C. Ho, Post metalation of solvothermally grown electroactive porphyrin metal–organic framework thin films, Chem. Commun. 51 (2015) 2414–2417.
[21] G. Dybwad, A sensitive new method for the determination of adhesive bonding between a particle and a substrate, J. Appl. Phys. 58 (1985) 2789–2790.
[22] A.L. Olsson, H.C. Van der Mei, H.J. Busscher, P.K. Sharma, Acoustic sensing of the bacterium–substratum interface using QCM-D and the influence of extracellular polymeric substances, J. Colloid Interface Sci. 357 (2011) 135–138.
[23] J.R. J. D′amour, K. Stålgren, C. Kanazawa, M. Frank, D. Rodahl Johannsmann, Capillary aging of the contacts between glass spheres and a quartz resonator surface, Phys. Rev. Lett. 96 (2006), 058301.
[24] W.D. Hunt, D.D. Stubbs, S.-H. Lee, Time-dependent signatures of acoustic wave biosensors, Proc. IEEE 91 (2003) 890–901.
[25] S.-H. Lee, D.D. Stubbs, J. Cairney, W.D. Hunt, Rapid detection of bacterial spores using a quartz crystal microbalance (QCM) immunoassay, IEEE Sens. J. 5 (2005) 737–743.
[26] F.L. Dickert, P. Lieberzeit, S.G. Miarecka, K.J. Mann, O. Hayden, C. Palfinger, Synthetic receptors for chemical sensors—subnano-and micrometre patterning by imprinting techniques, Biosens. Bioelectron. 20 (2004) 1040–1044.
[27] X. Gong, H. Noh, N.C. Gianneschi, O.K. Farha, Interrogating kinetic versus thermodynamic topologies of metal–organic frameworks via combined transmission electron microscopy and X-ray diffraction analysis, J. Am. Chem. Soc. 141 (2019) 6146–6151.
[28] N. Prasetya, C. Wöll, Removal of diclofenac by adsorption process studied in free-base porphyrin Zr-metal organic frameworks (Zr-MOFs, RSC Adv. 13 (2023) 22998–23009, https://doi.org/10.1039/D3RA03527A.
[29] H. Chen, Z. Chen, L. Zhang, P. Li, J. Liu, L.R. Redfern, S. Moribe, Q. Cui, R.Q. Snurr, O.K. Farha, Toward design rules of metal–organic frameworks for adsorption cooling: effect of topology on the ethanol working capacity, Chem. Mater. 31 (2019) 2702–2706.